Available online at www.sciencedirect.com
ScienceDirect
Trans. Nonferrous Met. Soc. China 30(2020) 1674−1686
Transactions of Nonferrous Metals Society of China
www.tnmsc.cn

Selective leaching of arsenic from copper converter flue dust by Na_2S and its stabilization with $Fe_2(SO_4)_3$

Amirhossein SHAHNAZI, Sadegh FIROOZI, Davoud HAGHSHENAS FATMEHSARI

Department of Mining and Metallurgical Engineering, Amirkabir University of Technology, 424 Hafez Ave., Tehran 15875-4413, Iran

Received 12 September 2019; accepted 6 May 2020

Abstract: The alkaline leaching of arsenic (As_2O_3) by Na_2S, together with its precipitation by $Fe_2(SO_4)_3$ was studied. Response surface methodology based on central composite design was employed to quantify and qualify the effect of pertinent factors and to develop statistical models for optimization purposes. Based on the obtained results, 89% of arsenic is removed from the dust under following optimum predicted conditions: Na_2S concentration of 100 g/L and solid to liquid ratio of 0.163 g/mL at 80 °C. It is found that solid to liquid ratio and Na_2S concentration are the significant factors influencing the leaching process. In the precipitation process, more than 99.93% of arsenic from the leaching solution is removed in the form of amorphous ferric arsenate, at pH 4.8 when Fe^{3+} to arsenic and H_2O_2 to arsenic molar ratios are set at 5:1 and 4:1, respectively. Also, Fe^{3+} to arsenic ratio and pH are the most significant factors, and the interaction between these terms is significant.

Key words: flue dust; arsenic; response surface methodology; alkaline leaching; precipitation

1 Introduction

During pyrometallurgical production of copper, a substantial amount of dusts containing copper and other impurities including arsenic, lead, zinc, and antimony are produced. Returning these dusts to the process results in the accumulation of impurities in the blister copper and makes the copper electrolysis process difficult [1]. More importantly, these dusts cannot be directly disposed, due to their very fine size since they are airborne and can be easily spread through a larger area, which is hazardous for the environment [2]. Arsenic, as a well-known toxic element, can be found widely in the waste materials of the copper industry [3]. Any process for the removal and safe stabilization of arsenic from the electrostatic precipitator (ESP) dust is not only necessary due to the utmost exploitation of its valuable metallic content, but also pivotal regarding the environmental concerns [4]. Propitiously, very fine size of these dusts facilitates the leaching process because it significantly enhances the rate of the leaching process.

Different strategies have been employed for the leaching of arsenic from various dusts including acidic and alkali leaching systems [5,6]. However, the primary deficiency of the acidic leaching is the dissolution of other metallic constituents present in the dusts including lead, copper and zinc. This means that acidic leaching is not selective and requires additional separation and purification processes [7,8]. On the other hand, alkali leaching systems such as Na_2S, NaOH or their mixtures, are selective with respect to arsenic in either sulfide [9] or oxide [6] forms. For instance, RUIZ et al [9] reported that 97% of the arsenic content of enargite could be dissolved at 80 °C by a mixture of Na_2S and NaOH solution while the copper content of enargite does not change. Also, LI et al [6] found

Corresponding author: Sadegh FIROOZI; E-mail: s.firoozi@aut.ac.ir
DOI: 10.1016/S1003-6326(20)65329-8

that 95% of arsenic content of smelter dusts (in the form of As_2O_3) can be dissolved by NaOH solution and only 20% of its Pb content enters into solution. They also showed that more than 92% of arsenic content of the dust could be dissolved by Na_2S solution at 90 °C and less than 37% of its zinc content enters into the solution [10].

After arsenic leaching, its safe stabilization is the next essential step. Arsenic can be found in the forms of arsenite and thioarsenite with the oxidation state of +3, and arsenate and thioarsenate with the oxidation state of +5 in the aqueous solutions. One of the most stable compounds of arsenic is scorodite ($FeAsO_4·2H_2O$) which is the product of the reaction between As^{5+} and Fe^{3+} at specific pH [11]. To precipitate $FeAsO_4$, not only pH adjustment is needed (e.g., the addition of $Ca(OH)_2$ or NaOH solutions [12,13]), but also arsenic content of the leaching solution should be in the form of As^{5+} by providing oxidative condition (e.g., aeration [14]). However, it should be pointed out that the use of $Ca(OH)_2$ solution, for pH adjustment, can also result in the formation of calcium arsenate depending on the values of pH and redox potential; this form of arsenic precipitation is not favorable since calcium arsenate slowly reacts with atmospheric CO_2 and eventually arsenic is released into the environment [13,15].

According to the above-mentioned leaching−precipitation strategies for arsenic leaching and stabilization, one essential step towards developing an effective removal−stabilization process is the use of a suitable methodology for optimization of the relevant parameters in both leaching and precipitation processes. The most significant factors influencing arsenic alkali leaching from dust sources are temperature, leachant concentration and solid to liquid ratio [16−18]. Also, H_2O_2 (as the oxidative agent) to arsenic molar ratio, Fe^{3+} to arsenic molar ratio and pH are also the significant factors affecting arsenic precipitation [19−22]. The appropriate choice of these factors is required if an effective arsenic leaching−stabilization process is to be proposed. The key point in such processes is that the level of each factor can be influenced by the other factors; i.e., there may be some interactions among influential factors.

A literature survey on arsenic leaching−precipitation studies indicates that “one-factor-at-a-time method” has been used to evaluate the relevant factors [23,24]. This methodology gives no information about the probable interactions among factors in a process. On the other hand, response surface methodology (RSM) can simultaneously consider several factors at different levels, develop an appropriate empirical model for the interaction among several factors and the response, and find the optimum value of each factor [25].

The present work aimed to evaluate the selective leaching and precipitation processes of arsenic in oxide form, As_2O_3, from the dust collected from ESP of a Pierce−Smith copper converter. While Na_2S and NaOH or their mixture have been abundantly used for leaching of sulfide form of arsenic [9,23,26,27], only in some limited works, Na_2S has been employed for the leaching of oxide form of arsenic. Moreover, while iron(III) sulfate is the common reagent for precipitation of arsenic from acidic leaching solutions [14,22,24,28], precipitation behavior of arsenic from the Na_2S leaching solution using $Fe_2(SO_4)_3$ is unknown. In both leaching and precipitation processes, RSM coupled with central composite design (CCD) was employed [29]:

(1) To develop a statistical relationship, albeit approximate, between responses and influential factors that can be used to predict response for a given set of factors.

(2) To determine the significance of factors and the interaction among relevant factors.

(3) To estimate the optimum levels of factors that result in the maximum (or minimum) response over a specific region of interest.

2 Experimental

2.1 Dust and reagents

Sodium sulfide hydrate ($Na_2S·xH_2O$, ~35%), iron(III) sulfate hydrate ($Fe_2(SO_4)_3·xH_2O$, 76%−82%) and H_2O_2 (30%) were obtained from Merck; the former reagent was employed for the preparation of leaching solution and the last two reagents were used in the precipitation experiments. Also, sodium hydroxide (NaOH, 97%) and sulfuric acid (H_2SO_4, 95%−98%) were purchased from Sigma−Aldrich and employed for pH adjustment in the precipitation experiments.

Three dust samples obtained from copper converter electrostatic precipitator (Shahrbabak Copper Complex, Khatoonabad, Kerman, Iran)

were well mixed and divided using riffle splitter. Arsenic content of the obtained mixture was determined using inductively coupled plasma optical emission spectrometry (ICP-OES, Varian, 720−ES) after complete digestion of the mixture by alkali fusion method. Besides, X-ray fluorescence spectrometry (XRF, Philips, PW1404) was employed for the estimation of the level of other elements in the mixture (Table 1). According to X-ray diffraction (XRD) analysis (PANalytical, X'Pert Pro MPD), arsenic was present in the mixture mainly in the form of As_2O_3; in addition, the other phases in the mixture were $PbSO_4$, SiO_2 and Cu_2S. Observation based on the field emission scanning electron microscopy (FESEM, TESCAN, Mira3−XMU) showed that mostly submicron spherical dust particles agglomerated into larger particles (Fig. 1). The mean particle size of the dust measured by static light scattering (SLS, Fritsch, Analysette 22) was 39 μm (Fig. 2).

Table 1 Chemical composition of ESP copper converter dust (Arsenic was measured using ICP analysis and other elements/compounds with XRF) (wt.%)

As	Pb	Cu	S	Zn	Fe
2.96	23.4	20.7	11.2	7.3	2.0
Sb	Al_2O_3	MgO	K_2O	SiO_2	LOI*
0.2	0.48	0.79	0.35	5.96	3.18

* Loss on ignition

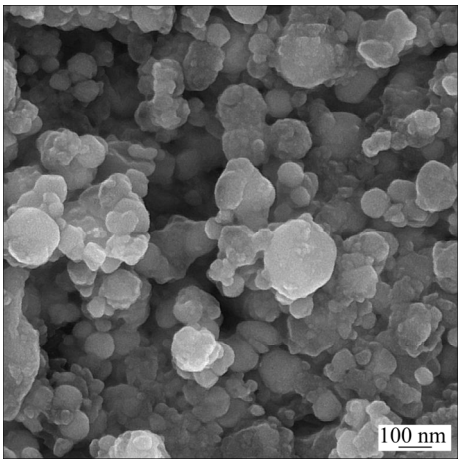

Fig. 1 FESEM image of convertor flue dust showing most submicron spherical dust particles agglomerated into larger particles

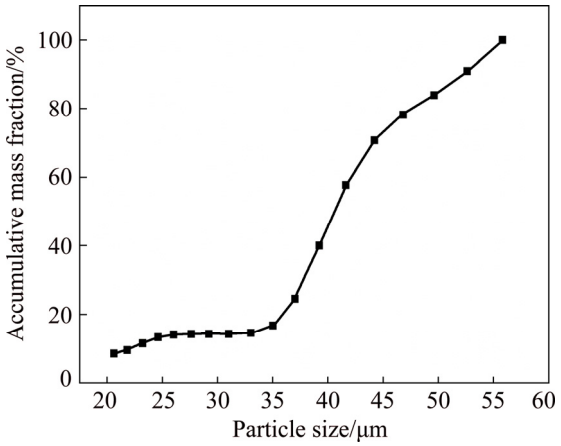

Fig. 2 Size distribution of copper converter flue dust (Mean size of particles is 39 μm and D_{80} is 48 μm)

2.2 Procedure

2.2.1 Alkali leaching

Leaching experiments were conducted in a 250 mL two-neck flat bottom flask immersed in a water bath. The system was stirred at 400 r/min for 4 h at different combinations of temperatures, Na_2S concentrations, and amounts of the dust mixture at a fixed solution volume of 100 mL. After each experimental run, the resulting pulps were filtered and the concentration of the dissolved elements in the solution was determined using ICP-OES (Varian, 720−ES). Furthermore, the final obtained leaching residues were analyzed by XRD method (PANalytical, X'Pert Pro MPD) for verification purposes. The leaching rate of arsenic (R) was estimated using Eq. (1) [30]:

$$R=\frac{cV}{mx}\times 100\% \quad (1)$$

where c and V are the arsenic concentration in leaching solution and volume of the solution, respectively; also, m and x are the dust mass and the mass fraction of arsenic in the dust mixture, respectively.

2.2.2 Precipitation

The precipitation step was performed on the leaching solution with the maximum leaching rate of arsenic (R) that was achieved from the set of factors proposed by the optimized leaching model. Initially, H_2O_2 was gradually introduced to the system for the complete conversion of As^{3+} to As^{5+} and then $Fe_2(SO_4)_3$ was added to the solution at ambient temperature under constant stirring at 400 r/min. During the $Fe_2(SO_4)_3$ addition, the pH of the solution was monitored (Portable Mettler Toledo pH meter) and adjusted by the use of NaOH and H_2SO_4. Finally, the precipitated arsenic was separated from the solution, and arsenic concentration of the obtained solution was

measured by ICP-OES analysis. The redox potential of the system (φ_H), with respect to the standard potential of hydrogen, was also measured by oxidation reduction potential meter (ORP meter, EUTECH instruments, Pt/saturated calomel electrode (SCE)). The chemical composition of arsenic precipitate was analyzed by XRF (Philips, PW1404) and XRD; in addition, the levels of copper, zinc, and lead were determined using inductively coupled plasma optical emission spectrometry (ICP-OES, Varian, 720−ES) after complete digestion of the mixture by alkali fusion method. The structure of the resulting precipitate was analyzed using XRD and the Fourier transform infrared spectroscopy (FTIR, Thermo scientific, Nicolet, iS10). Finally, toxicity characteristic of leaching procedure (TCLP) was carried out based on Environmental Protection Administration (EPA) standards in order to investigate the stability of arsenic precipitate [31].

Arsenic precipitation rate was calculated using Eq. (2) [32]:

$$P=\left(1-\frac{c_f}{c_i}\right)\times 100\% \quad (2)$$

where c_i and c_f are the initial (4293 mg/L) and final concentrations of arsenic solution, respectively.

2.3 Experimental design

RSM as a statistical approach has been widely used in various fields of materials science and metallurgical engineering [33−35]; in this approach, not only a correlation between the response and the factors for the prediction of response value can be established, but also the significance of the factors and their interactions can be identified and quantified.

Seventeen experimental runs consisting of eight star points (star distance was zero) and three center points and six axial points were chosen by the principle of RSM using Minitab® Release 17 for both arsenic leaching and precipitation processes. To develop a second-order polynomial model, a central composite design (CCD) with linear regression was employed to estimate the model coefficients of the three selected factors believed to influence R and P with each factor set at its high level (+1), low level (−1) and medium level (0). Amongst different factors, temperature (T), solid to liquid ratio (S/L) and Na_2S concentration ([Na_2S]) were selected in the leaching process, and H_2O_2 to arsenic molar ratios (H_2O_2/As), Fe^{3+} to arsenic molar ratios (Fe/As) and pH were selected in the precipitation process due to their higher importance reported in the literatures [11,21,23,36].

The levels used for these three factors, according to a CCD, are listed in Tables 2 and 3 for leaching and precipitation processes, respectively. The results for the response are reported as a mean value of each two responses in a randomized order to avoid systematic bias. Finally, a quadratic polynomial regression model (Eq. (3)) was employed to estimate and predict the response value over a range of input values [37]:

$$Y=b_0+\sum_{i=1}^{k}b_iX_i+\sum_{i=1}^{k}b_{ii}X_i^2+\sum_{i=1}^{k}\sum_{j=i+1}^{k}b_{ij}X_iX_j \quad (3)$$

where Y is the dependent response variable (i.e., R and P), b_0 is the intercept term, b_i, b_{ii}, and b_{ij} are the measures of the effect of variable X_i, X_i^2 and X_iX_j, respectively. X_i and X_j represent the independent variables and k is the number of these factors namely temperature (40−80 °C), solid to liquid ratio

Table 2 Central composite design arrangement and experimental results for arsenic leaching rate

Run No.	Factor			Measured As leaching rate, R/%
	T/ °C	(S/L)/ (g·mL^{-1})	[Na_2S]/ (g·L^{-1})	
1	40	0.15	50	38.3
2	80	0.15	50	47.0
3	40	0.25	50	8.6
4	80	0.25	50	12.6
5	40	0.15	100	78.3
6	80	0.15	100	83.5
7	40	0.25	100	72.6
8	80	0.25	100	68.0
9	40	0.20	75	51.1
10	80	0.20	75	56.3
11	60	0.15	75	60.0
12	60	0.25	75	35.0
13	60	0.20	50	25.0
14	60	0.20	100	80.1
15	60	0.20	75	57.0
16	60	0.20	75	59.0
17	60	0.20	75	55.0

Table 3 Central composite design arrangement and experimental results for arsenic precipitation rate

Run No.	Factor			Measured As precipitation rate, P/%
	H_2O_2/As	Fe/As	pH	
1	2:1	2.0:1	3.0	48.8
2	4:1	2.0:1	3.0	57.0
3	2:1	5.0:1	3.0	88.0
4	4:1	5.0:1	3.0	91.5
5	2:1	2.0:1	6.0	93.0
6	4:1	2.0:1	6.0	97.0
7	2:1	5.0:1	6.0	99.8
8	4:1	5.0:1	6.0	99.9
9	2:1	3.5:1	4.5	94.0
10	4:1	3.5:1	4.5	98.0
11	3:1	2.0:1	4.5	80.0
12	3:1	5.0:1	4.5	99.1
13	3:1	3.5:1	3.0	68.0
14	3:1	3.5:1	6.0	98.0
15	3:1	3.5:1	4.5	99.2
16	3:1	3.5:1	4.5	96.4
17	3:1	3.5:1	4.5	86.4

(0.15−0.25 g/mL) and Na_2S concentration (50−100 g/L in leaching process, and H_2O_2 to arsenic molar ratio (2:1−4:1), Fe to arsenic molar ratio (2:1−5:1), and pH (3−6) in precipitation process.

The analysis of variance (ANOVA) for the quadratic model was performed at 5% confidence level (i.e., P-value <0.05) [37]. The significance and the magnitude of the effect estimations for each variable and all their possible linear and quadratic interactions were also determined. The model was then used to predict the main effective factors. Finally, the predictions of the models were employed to reach the level of the factors that result in the maximum arsenic leaching and precipitation. The analysis was carried out using Minitab Release 17.

3 Results

3.1 Models fitting

Table 2 presents the leaching rate for 17 combinations of the factor levels. Similarly, Table 3 lists the measured arsenic precipitation rate. Also, the values of the regression coefficients for each factor in leaching and precipitation processes are presented in Table 4.

As it can be observed, the linear and quadratic terms are significant in both models indicating that the second-order polynomial model is necessary to represent the data. Based on P^*-values obtained from the regression coefficients (Table 4), the factors with a P^*-value lower than 0.05 were taken as the statistically significant factors in leaching or precipitation process. Thus, in the leaching process, the first order terms of S/L and [Na_2S], the second order term of S/L and the interaction between S/L and [Na_2S] were statistically significant. Moreover, in the precipitation process, the first order terms of Fe/As and pH, the second order term of pH and the interactive term of Fe/As and pH were statistically significant.

Table 4 Regression coefficients in coded values corresponding to leaching and precipitation processes

Leaching			Precipitation		
Factor	Regression coefficient	P^*-value	Factor	Regression coefficient	P^*-value
Constant	54.44	0.00	Constant	93.14	0.00
T	1.85	0.12	H_2O_2/As	1.98	0.15
S/L	−11.03	0.00	Fe/As	10.25	0.00
[Na_2S]	25.10	0.00	pH	13.44	0.00
T×T	1.18	0.58	(H_2O_2/As)×(H_2O_2/As)	3.51	0.18
(S/L)×(S/L)	−5.02	0.04	(Fe/As)×(Fe/As)	−2.94	0.25
[Na_2S]×[Na_2S]	0.03	0.99	pH×pH	−9.49	0.00
T×[Na_2S]	−1.51	0.24	(H_2O_2/As)×(Fe/As)	−1.07	0.45
T×(S/L)	−1.81	0.16	(H_2O_2/As)×pH	−0.95	0.51
(S/L)×[Na_2S]	5.36	0.00	(Fe/As)×pH	−8.00	0.00

Based on the estimated values of the regression coefficients (Table 4), two polynomial regression models were proposed (in un-coded values) as

$$R=-22.7+3.69(S/L)+0.320[Na_2S]-0.2008(S/L)\times(S/L)+0.0429(S/L)\times[Na_2S] \quad (4)$$

$$P=-119.0+34.13(Fe/As)+61.30pH-4.22pH\times pH-3.55(Fe/As)\times pH \quad (5)$$

The low values of P^* determined for the regression ($P^*<0.001$), and the insignificance of the model's lack of fit ($P^*>0.05$) show that both models are suitable and applicable (Table 5).

The main effect plots presented in Fig. 3 indicate that in the leaching process, an increase in the concentration of Na_2S from the lowest to highest values results in about three-fold increase in arsenic leaching rate (from ~25% to ~75%); however, increasing the S/L from its lowest to highest values leads to 25% decrease in arsenic leaching rate. These results are comparable to those reported by LI et al [21] in the case of arsenic in the form of complex lead arsenate leached by a mixture of Na_2S and NaOH. They also found that an increase in the level of Na_2S, in the NaOH (50 g/L)−Na_2S mixture, from 0 to 100 g/L increases arsenic leaching rate from 40% to 80% at 80 °C and S/L≈0.33 g/mL.

The main effect plot corresponding to temperature reveals that arsenic leaching rate slightly increases at elevated temperature, which means that the temperature is statistically insignificant within the studied range.

According to the main effect plots presented in Fig. 4, the most significant factors affecting arsenic precipitation rate are pH and Fe/As approximately with a similar effect; also, H_2O_2/As is not statistically significant within the studied range. The predicted results obtained from the arsenic precipitation main effect plots can be compared to

Table 5 ANOVA results corresponding to leaching and precipitation experiments

Parameter	Leaching				Precipitation			
	DF	adj SS	adj MS	P^*	DF	adj SS	adj MS	P^*
Regression	9	7909.4	878.8	0.00	9	3815.4	423.9	0.00
Linear	3	7550.9	2517	0.00	3	2896.2	965.4	0.00
Square	3	83.9	27.9	0.14	3	390.8	130.3	0.01
Interaction	3	274.6	91.5	0.01	3	528.5	176.2	0.00
Residual error	7	76.7	11		7	102.9	14.7	
Lack of fit	5	68.7	13.7	0.24	5	12.3	2.5	0.99
Pure error	2	8.0	4.0		2	90.6	45.3	
Total	16	7986.1			16	3918.3		

DF—Degrees of freedom; adj SS—Adjusted sum of squares; adj MS—Adjusted mean squares

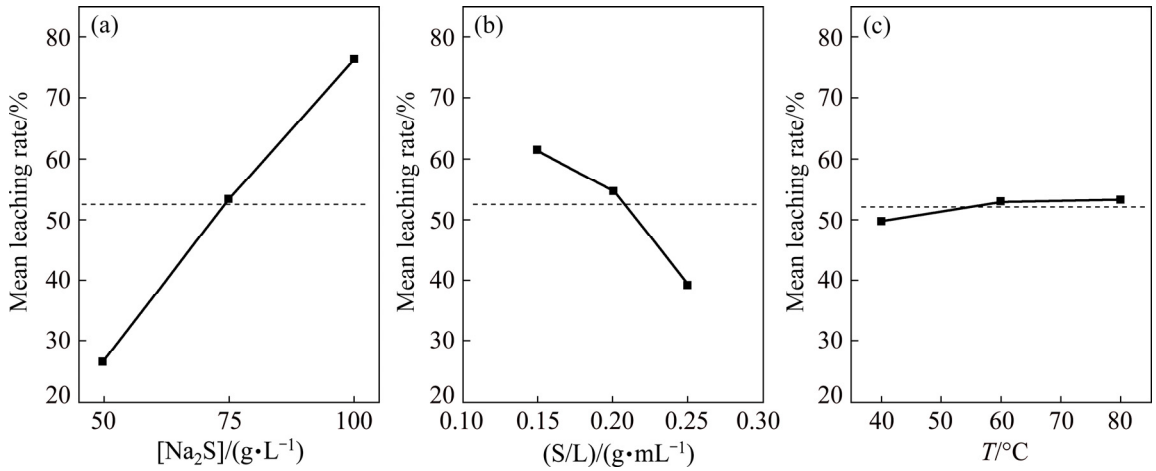

Fig. 3 Main effect plots for arsenic leaching efficiency from dust mixture by Na_2S leaching: (a) [Na_2S]; (b) S/L; (c) T

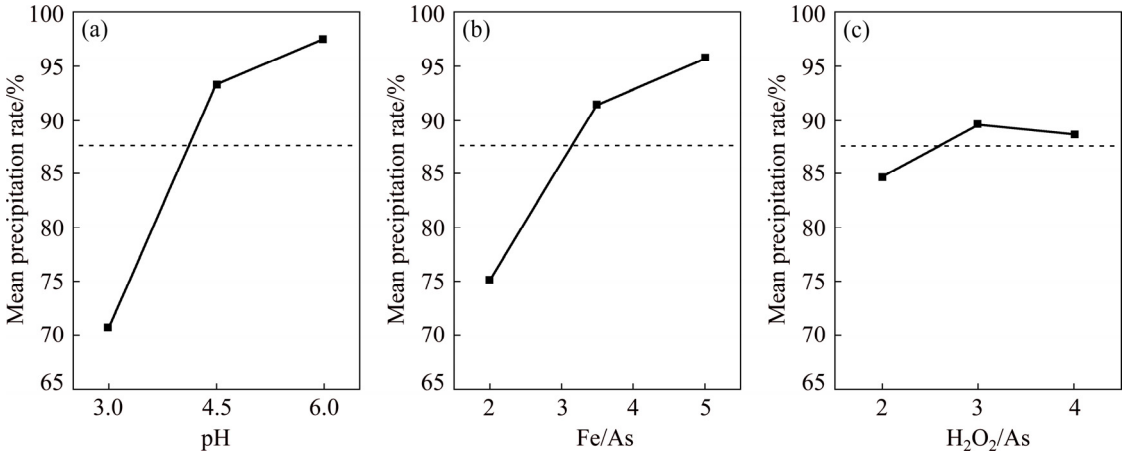

Fig. 4 Main effect plots of arsenic precipitation from leach liquor: (a) pH; (b) Fe/As; (c) H_2O_2/As

the results reported by WANG et al [11]. In arsenic precipitation process by $Fe_2(SO_4)_3$ from an alkaline solution, they found that more than 99% of arsenic content of the leaching solution can be precipitated with Fe/As of 1.5:1 within the pH range of 4.02−5.25.

3.2 Study of interactions among factors

Surface plots were used to examine statistically significant interactions. The surface plot presented in Fig. 5 illustrates the interaction between [Na_2S] and S/L in arsenic leaching process at 60 °C.

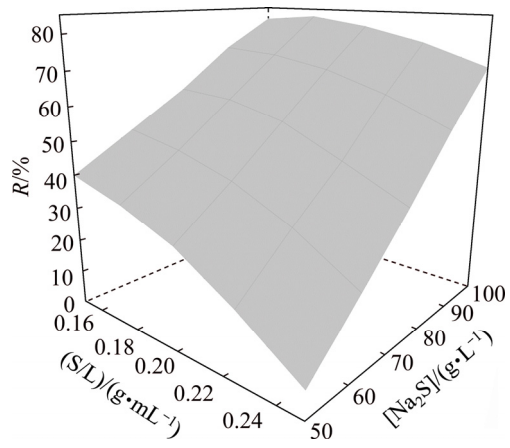

Fig. 5 Surface plot for arsenic leaching rate with respect to S/L and [Na_2S] at temperature of 60 °C

As it can be observed, with an increase in [Na_2S] from 50 to 100 g/L, there is a decrease in the slope of arsenic leaching rate with respect to S/L; in addition, at constant S/L, arsenic leaching rate increases by an increase in [Na_2S].

Figure 6 demonstrates the interactive effect of pH and Fe/As on arsenic precipitation rate at H_2O_2/As of 3:1. As it can be seen, with an increase in pH values from 3 to 6, there is a decrease in the slope of arsenic precipitation rate with respect to Fe/As.

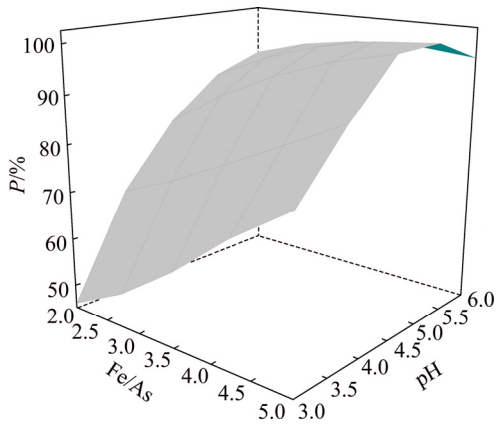

Fig. 6 Surface plot for arsenic precipitation rate with respect to Fe/As and pH value at H_2O_2/As value of 3

3.3 Optimization of factors in arsenic leaching and precipitation processes

Optimization of these three factors for obtaining the highest arsenic leaching rate in the first step and also, the maximum arsenic precipitation rate in the second step was carried out using the developed second-order polynomial models (Eqs. (4) and (5)). Based on this mathematical exercise, maximum arsenic leaching rate is predicted to be 83.9% under the following conditions: [Na_2S]=100 g/L, S/L=0.163 g/mL, and T=80 °C.

To confirm this prediction, and therefore the applicability of the proposed second-order model for further optimization exercises, a confirmation run (i.e., run at the predicted optimum level of the factors) was carried out and arsenic leaching rate of 88.6% was achieved; this can be taken as the confirmation of the suitability of the regression model for predictive purposes. The final solution obtained under these conditions with an arsenic concentration of 4293 mg/L was used as the starting solution for the precipitation process.

In precipitation step, the highest arsenic precipitation rate, at the pH=4.8, Fe/As=5:1 and H_2O_2/As=4:1, was predicted to be 100%. The confirmation run was carried out and values of 99.93% and 3 mg/L were achieved for arsenic precipitation rate and arsenic concentration in the final solution, respectively.

4 Discussion

Na_2S dissociates in the aqueous media according to Eq. (6) and at the pH of about 13, S^{2-} ions partially hydrolyze according to Eq. (7) [26]:

$$Na_2S \rightleftharpoons 2Na^+ + S^{2-} \quad (6)$$

$$S^{2-} + H_2O \rightleftharpoons HS^- + OH^-,\ K_{eq}=9.1\times10^{-3} \quad (7)$$

This means that the hydrolysis of Na_2S is not completed at pH around 13 and there is high enough S^{2-} in the aqueous solution for the dissolution of As_2O_3 based on Eq. (8) [27]:

$$As_2O_3(s) + 6S^{2-}(aq) + 3H_2O \rightleftharpoons 2AsS_3^{3-}(aq) + 6OH^-(aq) \quad (8)$$

Thioarsenite (AsS_3^{3-}) is a soluble form of arsenic and this reaction leads to the release of OH^-. Consequently, As_2O_3 can further react with OH^- (Eq. (9)) to form arsenite ion (AsO_3^{3-}) [38]:

$$As_2O_3(s) + 6OH^-(aq) \rightleftharpoons 2AsO_3^{3-}(aq) + 3H_2O \quad (9)$$

According to Eq. (8) and Eq. (9), As_2O_3 enters into the aqueous solution with an oxidation state of arsenic of +3 (in the form of AsO_3^{3-} and AsS_3^{3-}). Under oxidizing conditions, OH^- converts AsS_3^{3-} to AsO_3^{3-} as described by LI [39] who studied the dissolution of As_2O_3 by Na_2S. It is worthy of note that the level of OH^- in the system as well as the ratio of OH^- to As_2O_3 implicitly reflects the operational parameters namely [Na_2S] and S/L. In other words, the level of As_2O_3 in the system varies with the amount of solid entering to the system and the level of OH^- concentration directly depends on the concentration of Na_2S. This interrelationship appears in the interaction between [Na_2S] and S/L, as previously discussed in Section 3.2.

A comparison of XRD patterns of the dust mixture and the leaching residue (from optimized run: T=80 °C, [Na_2S]=100 g/L, S/L=0.163 g/mL) shows that the As_2O_3 peak at 2θ=18.6° is completely removed; however, the peak at 2θ=26° is still visible, which shows that some As_2O_3 is still present in the leached sample (Fig. 7). However, $PbSO_4$ and Cu_2S have remained unchanged during the leaching experiments. This is in agreement with the ICP-OES results of the leaching solution that shows the concentration of lead, copper, and zinc is negligible (i.e., selective leaching with respect to arsenic). Nonetheless, the ICP-OES results show 497 mg/L silicon and 213 mg/L antimony in the leaching solution, meaning partial dissolution of silicon and almost complete removal of antimony.

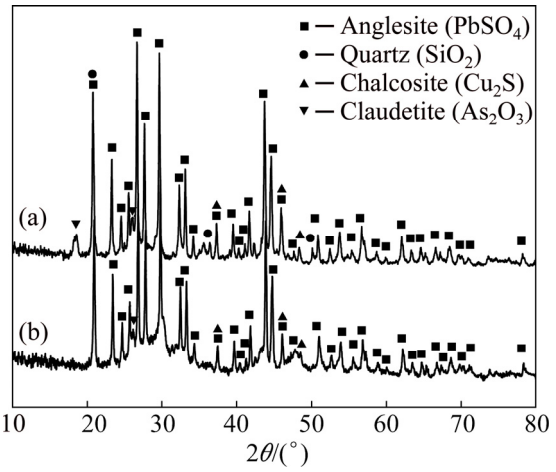

Fig. 7 Comparison between XRD patterns of dust (a) and leach residue obtained from optimized condition (S/L=0.163 g/mL, [Na_2S]=100 g/L and T=80 °C) (b)

For the effective precipitation of arsenic in the form of scorodite ($FeAsO_4\cdot2H_2O$), the conversion of AsO_3^{3-} (arsenic with the oxidation state of +3) into AsO_4^{3-} (arsenic with the oxidation state of +5) is essential by the use of an oxidant such as H_2O_2 [36]. The measured pH value of the solution after the leaching is 13.1. At this value, arsenic species in the oxidation state of +3 and +5 are predominantly in the form of $HAsO_3^{2-}$ and AsO_4^{3-}, respectively [40]. With the addition of H_2O_2, the oxidation reaction of $HAsO_3^{2-}$ can be presented as

$$HAsO_3^{2-}(aq)+H_2O_2(aq)\rightleftharpoons AsO_4^{3-}(aq)+H^+(aq)+H_2O \quad (10)$$

Equation (10) indicates that the oxidation of $HAsO_3^{2-}$ by H_2O_2 accompanies pH change as it is experimentally detected by a slight decrease in pH from 13.1 to 12.9. The precipitation reaction can be described as

$$AsO_4^{3-}(aq)+Fe^{3+}(aq)\rightleftharpoons FeAsO_4(s) \quad (11)$$

Therefore, the overall oxidative precipitation can be expressed as

$$HAsO_3^{2-}(aq)+Fe^{3+}(aq)+H_2O_2(aq)\rightleftharpoons FeAsO_4(s)+H^+(aq)+H_2O \quad (12)$$

By considering the equilibrium constant of Eq. (12) at constant temperature, the inter-relationship among Fe^{3+}, As^{5+} and H^+ (pH) can be established as

$$K_{eq}=\frac{[H^+]}{[HAsO_3^{2-}][H_2O_2][Fe^{3+}]} \quad (13)$$

where K_{eq} is the equilibrium constant and the activity of the solid product ($FeAsO_4$) is assumed to be 1. As it can be observed, pH of the system changes during oxidation reaction. On the other hand, the equilibrium constant of the redox reaction occurring in the system (Eq. (10)) can be presented as

$$K_{eq}=\frac{[AsO_4^{3-}][H^+]}{[HAsO_3^{2-}][H_2O_2]} \quad (14)$$

Regarding that $[AsO_4^{3-}]=[As^{5+}]$ and $[HAsO_3^{2-}]=[As^{3+}]$, the following relationship can be obtained:

$$\lg K_{eq}=\lg[As^{5+}]-\lg[As^{3+}]-pH-\lg[H_2O_2] \quad (15)$$

According to Nernst's equation, the standard potential difference (ε^0) is described as

$$\varepsilon^0=\frac{RT}{zF}\ln K_{eq} \quad (16)$$

And by combination of Eq. (15) and Eq. (16), the following relationship for the redox potential (φ_h) can be proposed:

$$\varphi_h=\varepsilon^0-\frac{RT}{zF}\ln K_{eq}=\varepsilon^0-\frac{RT}{zF}(\ln[As^{5+}]-\ln[As^{3+}]-2.3pH-\ln[H_2O_2]) \quad (17)$$

Equation (17) provides a correlation among φ_h, H_2O_2 concentration and As^{3+} initial concentration from a thermodynamic viewpoint. This correlation can be further identified by monitoring the change in the equilibrium oxidation−reduction potential (ORP) of the system. Figure 8 shows the variation of ORP (with respect to the standard hydrogen electrode) versus H_2O_2 concentration at constant As^{3+} initial concentration (4293 mg/L). As it can be observed, the ORP approaches a constant value near 130 mV at H_2O_2 concentration of 215 mmol/L from the initial value of −25 mV, which indicates the oxidation of As(III) [18]; this means that the addition of about 1.1 mL into 50 mL solution, significantly drops $[As^{5+}]/[As^{3+}]$ from an initial small value to a final value of $>10^5$. Thus, the H_2O_2/As is not statistically significant as previously mentioned in Section 3.1.

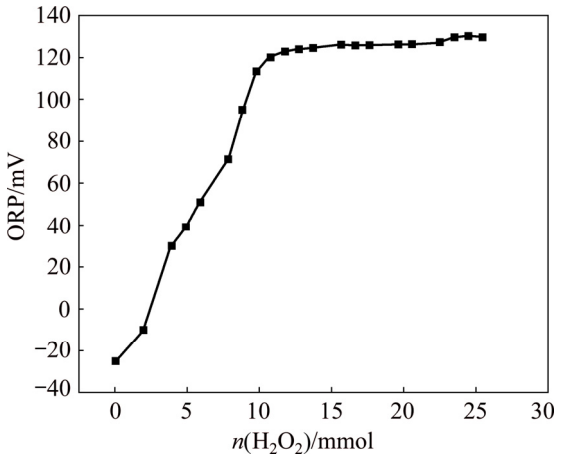

Fig. 8 Effect of H_2O_2 addition on ORP (vs saturated calomel electrode (SCE) to 50 mL solution with [As]= 4293 mg/L)

The levels of copper, lead and zinc are negligible in the precipitate obtained under optimum conditions (Table 6). Antimony is present in the precipitated product as well, which shows that this element has similar behavior to arsenic in the process. XRD pattern of the precipitated phase under optimum conditions (Fig. 9(a)) shows that only elemental sulfur is present as the crystalline product. Formation of elemental sulfur can be due to the reaction of excess $Fe_2(SO_4)_3$ or H_2O_2 with Na_2S that occurs when pH gets lowered to the desired value. After heating the precipitate at 200 °C in the air atmosphere for 1 h, the elemental sulfur is removed and as can be seen in Fig. 9(b), the remaining precipitate is fully amorphous.

It is worthy to note that crystalline scorodite cannot be achieved at ambient temperature during

Table 6 XRF and ICP analysis results of main and trace elements of precipitate under optimized condition (pH=4.8, Fe/As=5:1 and H_2O_2/As=4:1)

Element	XRF mass fraction/%	ICP mass fraction/10^{-6}
As	27.7	−
Sb	3.3	−
Fe	20.9	−
S	25.3	−
Si	0.1	−
Pb	−	39
Cu	−	332
Zn	−	172

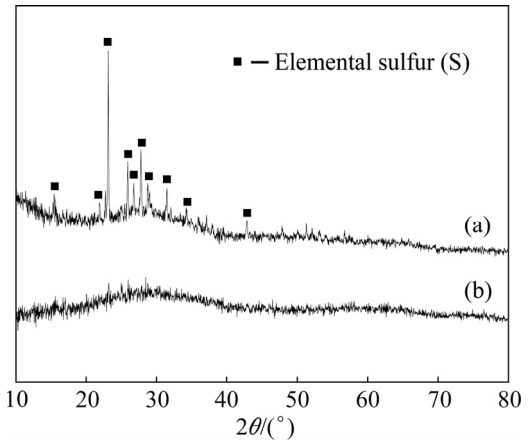

Fig. 9 XRD patterns of precipitate under optimized condition (pH=4.8, Fe/As=5:1 and H_2O_2/As=4:1): (a) As-recievied; (b) After heating at 200 °C for 1 h

the precipitation process [41]. However, wide background of such pattern may be attributed to amorphous arsenate as the expected phase under these conditions [42]; besides, the level of iron and arsenic in the precipitate is consistent with the stoichiometric ratio of arsenic to iron in ferric arsenate compound. Moreover, the FTIR spectrum of this sample (Fig. 10) conforms to be poor crystalline ferric arsenate ($FeAsO_4{\cdot}nH_2O$) reported by SONG et al [43]. The results of TCLP show the concentration of dissolved arsenic in the solution is 2 mg/L, which shows that the stability of the precipitate is acceptable. The stretching vibrations at 840 cm^{-1} belong to As—O—Fe, and the broad peak at about 3211 cm^{-1} is related to the —OH stretching mode in ferric hydroxide. The peak at 1628 cm^{-1} is related to H—OH bending vibration of water and the peak at 460 cm^{-1} is related to ferrihydrite.

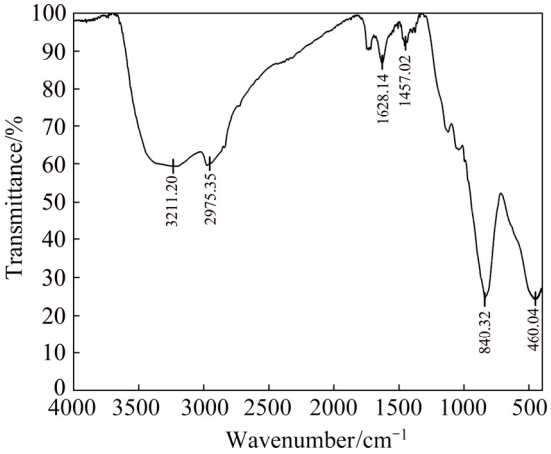

Fig. 10 FTIR spectrum of precipitate under optimum condition of pH=4.8, Fe/As=5:1 and H_2O_2/As=4:1 after heating in air at 200 °C for 1 h

Another important point regarding the interaction between Fe/As and pH is that in spite of previously reported such interaction [11,24], the mechanism of this interaction cannot be found by reference. The addition of $Fe_2(SO_4)_3$ into the solution results in arsenic precipitation via the formation of ferric arsenate and leads to a decrease in final pH. Based on these evidences, the following reaction can be proposed [22]:

$$Fe(SO_4)_{1.5}+H_3AsO_4+wH_2O\rightarrow FeAsO_4{\cdot}wH_2O+1.5H_2SO_4 \quad (18)$$

Generation of a strong acid is another reason for the decrease in pH value during precipitation process; i.e., by the addition of iron(III) sulfate into the system, pH drops from an initial value of 13.1 to 8.7−9.9, 5.6−6.2 and 4.3−5.6 when Fe/As molar ratio is 2:1, 3.5:1 and 5:1, respectively.

The result of the leaching and precipitation experiments may be used to propose a flow diagram for the selective removal and stabilization of arsenic from the copper converter ESP flue dust (Fig. 11). Leaching using Na_2S is beneficial in comparison with the acidic process where copper and zinc also enter into the leaching solution. Arsenic content of the leaching residue is 0.5% which is within the acceptable range to be recycled back to the copper production process; alternatively, this dust can be further treated for efficient separation and recovery of Pb and Zn. Moreover, lead, copper and zinc do not enter into the leaching solution, which simplifies the precipitation step and is advantageous for the recycling of the water back to the process.

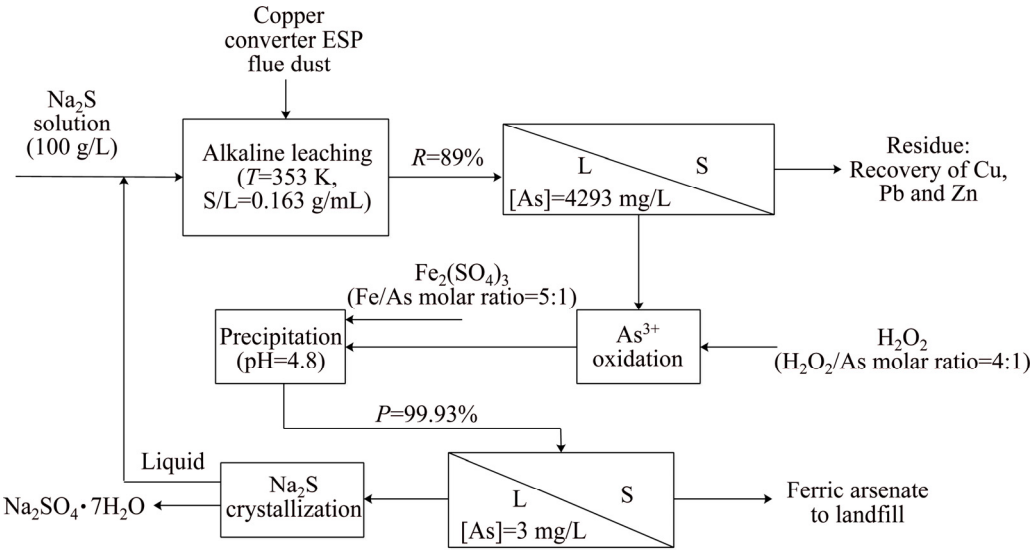

Fig. 11 Process flow sheet for alkaline leaching and chemical precipitation of arsenic in copper converter ESP flue dust (*R*: Arsenic leaching rate; *P*: Arsenic precipitation rate)

The precipitation step starts with the oxidation of As^{3+} to As^{5+} followed by the addition of $Fe_2(SO_4)_3$ to form the highly insoluble amorphous $FeAsO_4$. $Fe_2(SO_4)_3$ effectively reduces pH to the desired value eliminating the use of pH modifier. This is specifically advantageous in comparison with the precipitation of arsenic from an acidic medium that requires a considerable amount of pH modifiers such as calcium hydroxide, which results in the formation of undesired byproducts. The solution that contains Na_2SO_4 can be crystallized through cooling to precipitate Na_2SO_4 and then recycled back to the process.

5 Conclusions

(1) Based on the statistical approach, 89% arsenic is leached with Na_2S solution of 100 g/L and S/L ratio of 0.163 g/mL at 80 °C. S/L ratio and Na_2S concentration are the most significant factors influencing the leaching process and the interaction between them is statistically significant.

(2) The statistical analysis indicates that in arsenic stabilization, a precipitation rate higher than 99.93% is achieved at the pH level of 4.8, Fe/As molar ratio of 5:1 and H_2O_2/As molar ratio of 4:1. Results show that both Fe/As molar ratio and pH are the significant factors influencing the precipitation process and their interaction is meaningful.

Acknowledgments

The authors wish to thank the Shahrbabak Copper Complex, Kerman, Iran for providing the dust samples.

References

[1] SCHLESINGER M E, KING M J, DAVENPORT W G. Extractive metallurgy of copper [M]. 5th ed. Amsterdam: Elsevier, 2011.

[2] CSAVINA J, TAYLOR M P, FÉLIX O, RINE K P, SÁEZ A E, BETTERTON E A. Size-resolved dust and aerosol contaminants associated with copper and lead smelting emissions: Implications for emission management and human health [J]. Science of the Total Environment, 2014, 493: 750−756.

[3] JAROŠÍKOVÁ A, ETTLER V, MIHALJEVIČ M, DRAHOTA P, CULKA A, RACEK M. Characterization and pH-dependent environmental stability of arsenic trioxide-containing copper smelter flue dust [J]. Journal of Environmental Management, 2018, 209: 71−80.

[4] LANE D J, COOK N J, GRANO S R, EHRIG K. Selective leaching of penalty elements from copper concentrates: A review [J]. Minerals Engineering, 2016, 98: 110−121.

[5] KARIMOV K, NABOICHENKO S. Sulfuric acid leaching of high-arsenic dust from copper smelting [J]. Metallurgist, 2016, 60(3−4): 456−459.

[6] LI Y H, LIU Z H, LI Q H, LIU F P, LIU Z Y. Alkaline oxidative pressure leaching of arsenic and antimony bearing dusts [J]. Hydrometallurgy, 2016, 166: 41−47.

[7] WANG H J, LIU Z Y, LIU Z H, LI Y H, LI S W, ZHANG W H, LI Q H. Leaching of iron concentrate separated from kiln slag in zinc hydrometallurgy with hydrochloric acid and its mechanism [J]. Transactions of Nonferrous Metals Society of China, 2017, 27(4): 901−907.

[8] SHU Y X, CAO H Z, WU L K, HOU G Y, TANG Y P, ZHENG G Q. The comprehensive utilization of oxidative hydrochloric acid leaching of anode slime bearing fluorine, arsenic and antimony [J]. Hydrometallurgy, 2019, 183: 106−111.

[9] RUIZ M, GRANDON L, PADILLA R. Selective arsenic removal from enargite by alkaline digestion and water leaching [J]. Hydrometallurgy, 2014, 150: 20−26.

[10] GUO X Y, YU Y, JING S, TIAN Q H. Leaching behavior of metals from high-arsenic dust by NaOH−Na_2S alkaline leaching [J]. Transactions of Nonferrous Metals Society of China, 2016, 26(2): 575−580.

[11] WANG Y L, LV C C, XIAO L, FU G Y, LIU Y, YE S F, CHEN Y F. Arsenic removal from alkaline leaching solution using Fe(III) precipitation [J]. Environmental Technology, 2019, 40(13): 1714−1720.

[12] YUAN Z D, ZHANG D N, WANG S F, XU L Y, WANG K L, SONG Y, XIAO F, JIA Y F. Effect of hydroquinone-induced iron reduction on the stability of scorodite and arsenic mobilization [J]. Hydrometallurgy, 2016, 164: 228−237.

[13] RIVEROS P, DUTRIZAC J, SPENCER P. Arsenic disposal practices in the metallurgical industry [J]. Canadian Metallurgical Quarterly, 2001, 40(4): 395−420.

[14] CUI J, DU Y G, XIAO H X, YI Q S, DU D Y. A new process of continuous three-stage co-precipitation of arsenic with ferrous iron and lime [J]. Hydrometallurgy, 2014, 146: 169−174.

[15] ZHU Y N, ZHANG X H, XIE Q L, WANG D Q, CHENG G W. Solubility and stability of calcium arsenates at 25 °C [J]. Water, Air, and Soil Pollution, 2006, 169(1−4): 221−238.

[16] HAN J W, LIANG C, LIU W, QIN W Q, JIAO F, LI W H. Pretreatment of tin anode slime using alkaline pressure oxidative leaching [J]. Separation and Purification Technology, 2017, 174: 389−395.

[17] SEISKO S, AROMAA J, LATOSTENMAA P, FORSEN O, WILSON B, LUNDSTROM M. Pressure leaching of decopperized copper electrorefining anode slimes in strong acid solution [J]. Physicochemical Problems of Mineral Processing, 2017, 53: 465−474.

[18] XU Z F, QIANG L, NIE H P. Pressure leaching technique of smelter dust with high-copper and high-arsenic [J]. Transactions of Nonferrous Metals Society of China, 2010, 20(S): s176−s181.

[19] SHAO B B, GUAN Y Y, TIAN Z Y, GUAN X H, WU D L. Advantages of aeration in arsenic removal and arsenite oxidation by structural Fe(II) hydroxides in aqueous solution [J]. Colloids and Surfaces A: Physicochemical and Engineering Aspects, 2016, 506: 703−710.

[20] KATSOYIANNIS I A, VOEGELIN A, ZOUBOULIS A I, HUG S J. Enhanced As(III) oxidation and removal by combined use of zero valent iron and hydrogen peroxide in aerated waters at neutral pH values [J]. Journal of Hazardous Materials, 2015, 297: 1−7.

[21] LI Y H, LIU Z H, LI Q H, ZHAO Z W, LIU Z Y, ZENG L, LI L. Removal of arsenic from arsenate complex contained in secondary zinc oxide [J]. Hydrometallurgy, 2011, 109: 237−244.

[22] GOMEZ M, BECZE L, CUTLER J, DEMOPOULOS G. Hydrothermal reaction chemistry and characterization of ferric arsenate phases precipitated from $Fe_2(SO_4)_3$−As_2O_5−H_2SO_4 solutions [J]. Hydrometallurgy, 2011, 107: 74−90.

[23] AWE S A, SANDSTRÖM Å. Selective leaching of arsenic and antimony from a tetrahedrite rich complex sulphide concentrate using alkaline sulphide solution [J]. Minerals Engineering, 2010, 23(15): 1227−1236.

[24] JIA Y, DEMOPOULOS G P. Coprecipitation of arsenate with iron(III) in aqueous sulfate media: Effect of time, lime as base and co-ions on arsenic retention [J]. Water Research, 2008, 42(3): 661−668.

[25] MONTGOMERY D C. Design and analysis of experiments [M]. 9th ed. New York: John Wiley & Sons, 2017.

[26] DELFINI M, FERRINI M, MANNI A, MASSACCI P, PIGA L. Arsenic leaching by Na_2S to decontaminate tailings coming from colemanite processing [J]. Minerals Engineering, 2003, 16: 45−50.

[27] ANDERSON C, TWIDWELL L. The alkaline sulfide hydrometallurgical separation, recovery and fixation of tin, arsenic, antimony, mercury and gold [C]//International Symposium on Lead and Zinc Processing, Lead & Zinc. Durban, South Africa, PA: SAIMM, 2008: 121−132.

[28] DOERFELT C, FELDMANN T, ROY R, DEMOPOULOS G P. Stability of arsenate-bearing Fe(III)/Al(III) co-precipitates in the presence of sulfide as reducing agent under anoxic conditions [J]. Chemosphere, 2016, 151: 318−323.

[29] KHURI A I, MUKHOPADHYAY S. Response surface methodology [J]. Wiley Interdisciplinary Reviews: Computational Statistics, 2010, 2(2): 128−149.

[30] ZHOU K G, TENG C Y, ZHANG X K, PENG C H, CHEN W. Enhanced selective leaching of scandium from red mud [J]. Hydrometallurgy, 2018, 182: 57−63.

[31] PENG B, LIE J, MIN X B, CHAI L Y, LIANG Y J, YOU Y. Physicochemical properties of arsenic-bearing lime–ferrate sludge and its leaching behaviors [J]. Transactions of Nonferrous Metals Society of China, 2017, 27(5): 1188−1198.

[32] BULUT G, YENIAL Ü, EMIROĞLU E, SIRKECI A A. Arsenic removal from aqueous solution using pyrite [J]. Journal of Cleaner Production, 2014, 84: 526−532.

[33] WATSON M A, TUBIĆ A, AGBABA J, NIKIĆ J, MALETIĆ S, JAZIĆ J M, DALMACIJA B. Response surface methodology investigation into the interactions between arsenic and humic acid in water during the coagulation process [J]. Journal of Hazardous Materials, 2016, 312: 150−158.

[34] NADIMI H, AMIRJANI A, FATMEHSARI D H, FIROOZI S, AZADMEHR A. Effect of tartrate ion on extraction behavior of Ni and Co via D2EHPA in sulfate media [J]. Minerals Engineering, 2014, 69: 177−184.

[35] LIU H, ZHANG Y M, HUANG J, LIU T, XUE N N, SHI Q H. Optimization of vanadium(IV) extraction from stone coal leaching solution by emulsion liquid membrane using response surface methodology [J]. Chemical Engineering Research and Design, 2017, 123: 111−119.

[36] LI Y H, LIU Z H, LI Q H, ZHAO Z W, LIU Z Y, ZENG L. Removal of arsenic from Waelz zinc oxide using a mixed NaOH−Na_2S leach [J]. Hydrometallurgy, 2011, 108: 165−170.

[37] HAGHSHENAS D F, BONAKDARPOUR B, ALAMDARI

E K, NASERNEJAD B. Optimization of physicochemical parameters for bioleaching of sphalerite by *Acidithiobacillus ferrooxidans* using shaking bioreactors [J]. Hydrometallurgy, 2012, 111: 22−28.

[38] ZHENG Y J, XIAO F X, WANG Y, LI C H, XU W, JIAN H S, MA Y T. Industrial experiment of copper electrolyte purification by copper arsenite [J]. Journal of Central South University of Technology, 2008, 15(2): 204−208.

[39] LI W. Synthesis and solubility of arsenic tri-sulfide and sodium arsenic oxy-sulfide complexes in alkaline sulfide solutions [D]. Vancouver: University of British Columbia, 2013: 1−123.

[40] SHARMA V K, SOHN M. Aquatic arsenic: Toxicity, speciation, transformations, and remediation [J]. Environment International, 2009, 35(4): 743−759.

[41] LE BERRE J, GAUVIN R, DEMOPOULOS G. A study of the crystallization kinetics of scorodite via the transformation of poorly crystalline ferric arsenate in weakly acidic solution [J]. Colloids and Surfaces A: Physicochemical and Engineering Aspects, 2008, 315(1−3): 117−129.

[42] CHEN Y, LIAO T, LI G B, CHEN B Z, SHI X C. Recovery of bismuth and arsenic from copper smelter flue dusts after copper and zinc extraction [J]. Minerals Engineering, 2012, 39: 23−28.

[43] SONG J, JIA S Y, YU B, WU S H, HAN X. Formation of iron (hydr)oxides during the abiotic oxidation of Fe(II) in the presence of arsenate [J]. Journal of Hazardous Materials, 2015, 294: 70−79.

Na_2S 选择性浸出铜转炉烟灰中的砷及 $Fe_2(SO_4)_3$ 稳定化砷

Amirhossein SHAHNAZI, Sadegh FIROOZI, Davoud HAGHSHENAS FATMEHSARI

Department of Mining and Metallurgical Engineering, Amirkabir University of Technology, 424 Hafez Ave., Tehran 15875-4413, Iran

摘　要：研究砷(As_2O_3)的 Na_2S 碱性浸出，以及用 $Fe_2(SO_4)_3$ 沉淀砷。采用基于中心组合设计的响应面法对相关因素的影响进行定量和定性分析，提出用于参数优化的统计模型。结果表明，在 Na_2S 浓度 100 g/L，固液比 0.163 g/mL 和温度 80 °C 的最优预测条件下，89%的砷可从烟灰中去除。研究发现，固液比和 Na_2S 浓度是影响浸出过程的显著因素。在沉淀过程中，当 pH 为 4.8、Fe^{3+}与砷的摩尔比和 H_2O_2 与砷的摩尔比分别为 5:1 和 4:1 时，浸出液中 99.93%以上的砷以无定形砷酸铁的形式被除去。Fe^{3+}与砷的摩尔比和 pH 值为最显著因素，而且他们之间的相互作用也是显著的。

关键词：烟灰；砷；响应面法；碱性浸出；沉淀

(Edited by Bing YANG)